Commun Nonlinear Sci Numer Simulat 17 (2012) 1201–1210

Contents lists available at SciVerse ScienceDirect

Commun Nonlinear Sci Numer Simulat

journal homepage: www.elsevier.com/locate/cnsns

The time-splitting Fourier spectral method for the coupled Schrödinger–Boussinesq equations

Dongmei Bai *, Jianli Wang

College of Science, China University of Mining and Technology, Xuzhou 221116, China

ARTICLE INFO

Article history:
Received 4 March 2011
Received in revised form 1 August 2011
Accepted 7 August 2011
Available online 16 August 2011

Keywords:
Coupled Schrödinger–Boussinesq equations
Time-splitting
Fourier spectral method

ABSTRACT

The periodic initial boundary value problem of the coupled Schrödinger–Boussinesq equations is studied by the time-splitting Fourier spectral method. A time-splitting spectral discretization for the Schrödinger-like equation is applied, while a Crank–Nicolson/leap-frog type discretization is utilized for time derivatives in the Boussinesq-like equation. Numerical tests show that the time-splitting Fourier spectral method provides high accuracy for the coupled Schrödinger–Boussinesq equations.

1. Introduction

The coupled nonlinear partial differential equations (NPDEs) have often been proposed to describe the interaction of long waves with short wave packets in nonlinear dispersive media. For example, the coupled Schrödinger–Boussinesq (SB) system [1–5]

$$i\varepsilon u_t + \frac{3}{2}u_{xx} = \frac{1}{2}vu, \quad x \in \mathbf{R} > 0, \quad t > 0, \tag{1.1}$$

$$v_{tt} - v_{xx} - v_{xxxx} - (v^2)_{xx} = \frac{1}{4}(|u|^2)_{xx}, \quad x \in \mathbf{R} > 0, \quad t > 0, \tag{1.2}$$

govern the nonlinear development of modulational instabilities associated with Langmuir field amplitude coupled to intense electromagnetic waves in dispersive media such as plasmas. The complex-valued function u represents the short wave amplitude, the real-valued function v represents the long wave amplitude, and the subscripts t and x denote partial differentiation with respect to time and space, respectively. $\varepsilon > 0$, is a parameter indicating the mass ratio between the electron number and the ion number. In Ref. [2], the system (1.1) and (1.2) has appeared as a special case of a more general system governing the stationary propagation of coupled nonlinear upper-hybrid and magnetosonic waves in magnetized plasma. N-soliton solutions to (1.1) and (1.2) have been obtained in Ref. [6]. The study on soliton solutions has been the subject of research for many years and has motivated a series of work in physics and mathematics. Rao [7] studied solitary wave solutions in sech $\times$ tanh and sech^2 forms as well as sech and sech^2 forms using a power series expansion method. Wang et al. [8] examined these coupled equations using an ansatz making method and obtained a separate variety of solitary solutions in the form of sech^2 and sech^2 type solutions in 1993. Panigrahy and Dash [9] studied them again by using a mixing exponential method and obtained some solutions in A + sech^2 and B + sech^2 forms (A, B are real constants) in 1999. These solutions are not general and by no means exhaust all possibilities. They are only some particular solutions within some

* Corresponding author.
E-mail address: dmbai@cumt.edu.cn (D. Bai).

1007-5704/$ - see front matter © 2011 Elsevier B.V. All rights reserved.
doi:10.1016/j.cnsns.2011.08.012

specific parameters choices. Numerical methods are important tools to understand the feature of the NPDEs and to obtain possible physical applications. However, numerical methods and simulation for the SB system in the literature remain very limited. Therefore, some numerical work concerning this coupled SB equations would seem highly desirable.

We intend to study the coupled SB equations by the time-splitting Fourier spectral (TSFS) method. Comparing with our previous work about the coupled Schrödnger–KdV equations [10], we note that the Boussinesq equation has fourth-order space and second-order time derivatives whereas the KdV equation has third-order space and first-order time derivative terms, which makes it possible to allow bidirectional propagation [3–5]. The method of the time-splitting is a familiar technique in solving the nonlinear differential equation, as in [11–14], the initial and boundary-value problem is decomposed into linear and nonlinear subproblems. Different from the method in [10], the fourier spectral method is employed for the spatial discretizations of both linear and nonlinear subproblems. While the linear subproblem is treated exactly. The orthogonal trigonometric polynomial function provide a reasonable and consistent basis and offer high accuracy for the construction of a large variety of numerical problems [15,16]. We can get ordinary differential equations (ODEs) through the Fourier pseudospectral discretization to the Boussinesq equation. Numerical experiments are conducted to verify the accuracy and efficiency of our method.

2. Properties of the Schrödinger–Boussinesq equations

In this section, we will review some properties of the SB Eqs. (1.1) and (1.2) including conservation laws and solitary wave solution.

(a) *Conservation laws*. The SB equations have at least three invariants which are the Langmuir plasmon number:

$$I_u(t) = \int_{\mathbf{R}} |u|^2 dx \equiv \int_{\mathbf{R}} |u_0|^2 dx = I_u(0), \quad t \geqslant 0, \tag{2.1}$$

the total perturbed number density:

$$I_v(t) = \int_{\mathbf{R}} v dx = \int_{\mathbf{R}} v_0(x) dx = I_v(0), \quad t \geqslant 0, \tag{2.2}$$

and the total energy:

$$I_H(t) = \int_{\mathbf{R}} [(w_x)^2 + \frac{3}{2}|u_x|^2 + v^2 - (v_x)^2 + \frac{2}{3}v^3 + \frac{1}{2}v|u|^2] dx = I_H(0), \quad t \geqslant 0, \tag{2.3}$$

where w is a auxiliary variable which has the following form

$$w_{xx} = v_t. \tag{2.4}$$

Physically, these integral invariants are useful in analyzing the allowed or the forbidden interactions between the nonlinear entities obtained as solutions of (1.1) and (1.2).

(b) *Solitary-wave solution*. When the parameter $\varepsilon = 1$ in (1.1), the SB equations admits the solitary-wave solutions [17,18]

$$u(x,t) = \pm 8\sqrt{3}\lambda \operatorname{sech}(\rho\xi)\tanh(\rho\xi)\exp(i[kx + \omega t]), \tag{2.5}$$

$$v(x,t) = -6\lambda \operatorname{sech}^2(\rho\xi), \tag{2.6}$$

where $\xi = x - mt$, ρ, λ, k and ω are constants. m is the normalized speed called the "Mach number" of the stationary frame. The solutions (2.5) and (2.6) are sometimes collectively referred to as the "C-soliton" solutions.

(c) *Plane-wave solution*. The SB equations admit the plane-wave solutions [19]:

$$v(x,t) = d, \quad u(x,t) = A\exp(i(k_0 x - \omega_0 t)), \quad x \in \mathbf{R}, \quad t \geqslant 0, \tag{2.7}$$

where A, k_0, ω_0 and d are constants. ω_0 satisfies the relation $\omega_0 = \frac{d+3k_0^2}{2\varepsilon}$.

3. Numerical methods for the Schrödinger–Boussinesq equations

We present an efficient and accurate numerical methods for the SB Eqs. (1.1) and (1.2) in this section. For simplicity of notation, we shall introduce the method for the SB system with initial and boundary conditions. The problem becomes

$$i\varepsilon u_t + \frac{3}{2}u_{xx} = \frac{1}{2}vu, \quad a < x < b, \quad t > 0, \tag{3.1}$$

$$v_{tt} - v_{xx} - v_{xxxx} - (v^2)_{xx} = \frac{1}{4}(|u|^2)_{xx}, \quad a < x < b, \quad t > 0, \tag{3.2}$$

$$u(a,t) = u(b,t), \quad v(a,t) = v(b,t), \quad t \geqslant 0, \tag{3.3}$$

$$u(x,0) = \gamma_0(x), \quad v(x,0) = \eta_0(x), \quad v_t(x,0) = \eta_1(x), \quad a \leqslant x \leqslant b, \tag{3.4}$$

where $\gamma_0(x)$, $\eta_0(x)$ and $\eta_1(x)$ satisfy the periodic boundary condition (3.3) with the period $L = b - a$.

The proof of the existence of analytical solutions of (3.1)–(3.4) is presented in [11]. Assumed that the initial value $\gamma_0(x)$, $\eta_0(x)$ and $\eta_1(x)$ satisfy some smooth conditions, the maximum-norm of solutions u and v are bounded. Moreover, we supplement (3.1)–(3.4) by imposing the compatibility condition

$$\int_a^b \eta_1(x)dx = 0. \tag{3.5}$$

In some cases, the periodic boundary conditions (3.4) may be replaced by the homogeneous Dirichlet boundary conditions

$$u(a,t) = u(b,t) = 0, \quad v(a,t) = v(b,t) = 0, \quad t \geqslant 0, \tag{3.6}$$

If the spatial period is, for convenience, normalized to $[0,2\pi]$ using the transformation $\tilde{x} = 2\pi(x-a)/(b-a)$, the Eqs. (3.1)–(3.4) become

$$i\varepsilon u_t + \frac{3}{2}\alpha u_{\tilde{x}\tilde{x}} = \frac{1}{2}vu, \quad 0 \leqslant \tilde{x} \leqslant 2\pi, \quad t > 0, \tag{3.7}$$

$$v_{tt} - \alpha v_{\tilde{x}\tilde{x}} - \alpha^2 v_{\tilde{x}\tilde{x}\tilde{x}\tilde{x}} - \alpha(v^2)_{\tilde{x}\tilde{x}} = \frac{\alpha}{4}(|u|^2)_{\tilde{x}\tilde{x}}, \quad 0 \leqslant \tilde{x} \leqslant 2\pi, \quad t > 0, \tag{3.8}$$

$$u(\tilde{x},0) = \gamma_0(\tilde{x}), v(\tilde{x},0) = \eta_0(\tilde{x}), \quad v_t(\tilde{x},0) = \eta_1(\tilde{x}), \quad 0 \leqslant \tilde{x} \leqslant 2\pi, \tag{3.9}$$

$$u(0,t) = u(2\pi,t), \quad v(0,t) = v(2\pi,t), \quad t \geqslant 0, \tag{3.10}$$

where $\alpha = (b-a)^2/(4\pi^2)$.

3.1. Discretization

We choose the spatial mesh size $h = \Delta\tilde{x} > 0$ with $h = 2\pi/M$ for M being an even positive integer, the time step size being $\Delta t > 0$ and let the grid points and the time steps be

$$\tilde{x}_j = \frac{2\pi j}{M}, \quad j = 0,1,\ldots,M; \quad t_n = n\Delta t, \quad n = 0,1,2,\ldots.$$

Let u_j^n and v_j^n be the approximation of $u(\tilde{x}_j,t_n)$ and $v(\tilde{x}_j,t_n)$, respectively. Furthermore, let u^n and v^n be the solution vector at time $t = t_n = n\Delta t$ with the components of $u(\tilde{x}_j,t_n)$ and $v(\tilde{x}_j,t_n)$, respectively.

From t_n to t_{n+1}, the first Schrödinger-like Eq. (3.7) is solved in two splitting steps. One solves first

$$i\varepsilon u_t + \frac{3}{2}\alpha u_{\tilde{x}\tilde{x}} = 0 \tag{3.11}$$

for the time step of length τ, followed by solving

$$i\varepsilon u_t = \frac{1}{2}uv, \tag{3.12}$$

for the same time step. Eq. (3.11) will be discretized in space by Fourier spectral method and integrated in time exactly. For each fixed $\tilde{x} \in [0,2\pi]$, integrating (3.12) from t_n to t_{n+1}, and then approximating the integral on $[t_n,t_{n+1}]$ via the rectangular rule, we obtain that

$$u(\tilde{x},t_{n+1}) = \exp\left[\int_{t_n}^{t_{n+1}}\left(-\frac{i}{2\varepsilon}v(\tilde{x},s)\right)ds\right]u(x,t_n) = \exp\left[-\frac{i}{4\varepsilon}\tau(v(\tilde{x},t_n) + v(\tilde{x},t_{n+1}))\right]u(\tilde{x},t_n), \quad 0 \leqslant \tilde{x} \leqslant 2\pi. \tag{3.13}$$

The spatial derivative is approximated by pseudospectral method. For simply explanation, we introduce a generalized function $f(\tilde{x},t)$ and assume that $f(\tilde{x},t)$ satisfies the periodic boundary condition $f(0,t) = f(2\pi,t)$ for $(\tilde{x},t) \in \mathbf{R} \times [0,T]$. From t_n to t_{n+1}, the discrete Fourier transformation of the sequence $\{f_j\}$ is defined as

$$\hat{f}_k(t) = F_k[f_j(t)] = \sum_{j=0}^{M-1} f_j(t)\exp(-ik\tilde{x}_j), \quad k = -\frac{M}{2},\ldots,\frac{M}{2}-1. \tag{3.14}$$

The inversion formula for the discrete Fourier transform (3.14) is

$$f_j(t) = F_j^{-1}[\hat{f}_k(t)] = \frac{1}{M}\sum_{k=-M/2}^{M/2-1}\hat{f}_k(t)\exp(ik\tilde{x}_j), \quad j = 0,1,2,\ldots,M-1. \tag{3.15}$$

Here, F denotes the discrete Fourier transform and F^{-1} its inverse. These transforms can be realized efficiently via a fast Fourier transform algorithm.

3.2. First-order splitting scheme for the Schrödinger-like equation

The Schrodinger-like Eq. (3.7) is divided into Eqs. (3.11) and (3.12) in one time step. The Eq. (3.11) is discretized in space by spectral method and integrated in time exactly. The Eq. (3.12) is solved by (3.13). Then, we get the detailed first-order splitting scheme for Eq. (3.7)

$$u_j^* = \frac{1}{M}\sum_{k=-M/2}^{M/2-1} \exp\left(\frac{3\alpha i}{2\varepsilon}(ik)^2\tau\right)(\hat{u}^n)_k \exp(ik\tilde{x}_j), \quad j = 0,1,2,\ldots,M-1, \tag{3.16}$$

$$u_j^{n+1} = \exp\left(-\frac{i}{4\varepsilon}\left(v_j^n + v_j^{n+1}\right)\cdot\tau\right)\cdot u_j^*, \quad j = 0,1,2,\ldots,M-1, \tag{3.17}$$

where $(\hat{u}^n)_k$ the Fourier coefficients of u^n, with

$$u_j^0 = \gamma_0(\tilde{x}_j), \quad v_j^0 = \eta_0(\tilde{x}_j), \quad j = 0,1,2,\ldots,M-1. \tag{3.18}$$

3.3. Second-order splitting scheme for the Schrödinger-like equation

From t_n to t_{n+1}, we split the Schrödinger-like Eq. (3.7) via Strang splitting

$$u_j^* = \frac{1}{M}\sum_{k=-M/2}^{M/2-1} \exp\left(\frac{3\alpha i}{4\varepsilon}(ik)^2\tau\right)(\hat{u}^n)_k \exp(ik\tilde{x}_j), \quad j = 0,1,2,\ldots,M-1, \tag{3.19}$$

$$u_j^{**} = \exp\left(-\frac{i}{4\varepsilon}\left(v_j^n + v_j^{n+1}\right)\cdot\tau\right)\cdot u_j^*, \quad j = 0,1,2,\ldots,M-1, \tag{3.20}$$

$$u_j^{n+1} = \frac{1}{M}\sum_{k=-M/2}^{M/2-1} \exp\left(\frac{3\alpha i}{4\varepsilon}(ik)^2\tau\right)(\hat{u}^{**})_k \exp(ik\tilde{x}_j), \quad j = 0,1,2,\ldots,M-1, \tag{3.21}$$

where $(\hat{u}^{**})_k$ the Fourier coefficients of u^{**}.

3.4. Pseudospectral scheme for the Boussinesq-like equation

For the Boussinesq Eq. (3.8), we approximate spatial derivatives using the pseudospectral method. Denote $D_{\tilde{x}\tilde{x}}$, a spectral differential operator approximating $\partial_{\tilde{x}\tilde{x}}$, which is defined as $D_{\tilde{x}\tilde{x}}f = F^{-1}[(ik)^2F(f)]$. Followed by application of a Crank–Nicolson/leap-frog method for linear/nonlinear terms for time derivatives:

$$\begin{aligned}&\frac{v_j^{n+1} - 2v_j^n + v_j^{n-1}}{\tau^2} - \alpha D_{\tilde{x}\tilde{x}}(\beta v^{n+1} + (1-2\beta)v^n + \beta v^{n-1})_{\tilde{x}=\tilde{x}_j}\\ &- \alpha^2 D_{\tilde{x}\tilde{x}\tilde{x}\tilde{x}}(\beta v^{n+1} + (1-2\beta)v^n + \beta v^{n-1})_{\tilde{x}=\tilde{x}_j} - \alpha D_{\tilde{x}\tilde{x}}(\beta(v^{n+1})^2 + (1-2\beta)(v^n)^2 + \beta(v^{n-1})^2)_{\tilde{x}=\tilde{x}_j} = \frac{\alpha}{4}D_{\tilde{x}\tilde{x}}(|u^n|^2)_{\tilde{x}=\tilde{x}_j},\end{aligned} \tag{3.22}$$

where $0 \leqslant \beta \leqslant 1/2$ is a constant. The discretization (3.22) to (3.9) is explicit and linear for $\beta = 0$, while the discretization is implicit and nonlinear for $0 < \beta \leqslant 1/2$. Notice that

$$v_j^n = \frac{1}{M}\sum_{k=-M/2}^{M/2-1} (\hat{v}^n)_k \exp(ik\tilde{x}_j), \quad j = 0,1,2,\ldots,M. \tag{3.23}$$

Plugging (3.23) into (3.22) and using the orthogonality of the Fourier function, we obtain

$$\begin{aligned}&\frac{(\hat{v}^{n+1})_k - 2(\hat{v}^n)_k + (\hat{v}^{n-1})_k}{\tau^2} - (\alpha^2k^4 - \alpha k^2)\left[\beta(\hat{v}^{n+1})_k + (1-2\beta)(\hat{v}^n)_k + \beta(\hat{v}^{n-1})_k\right]\\ &+ \alpha k^2 F_k\left[\beta(v^{n+1})^2 + (1-2\beta)(v^n)^2 + \beta(v^{n-1})^2\right] = -\frac{\alpha}{4}k^2F_k(|u^n|^2),\end{aligned} \tag{3.24}$$

for $t_n \leqslant t \leqslant t_{n+1}$, $n \geqslant 0$.

The initial conditions are discretized as

$$u_j^0 = \gamma_0(\tilde{x}_j), \quad v_j^0 = \eta_0(\tilde{x}_j), \quad \frac{v_j^1 - v_j^{-1}}{2\tau} = \eta_1(\tilde{x}_j) \quad j = 0,1,\ldots,M-1. \tag{3.25}$$

From the Taylor formulation and the Eq. (3.8), it implies that

$$(\hat{v}^1)_k = (\hat{v}^0)_k + \tau(\hat{v}_t^0)_k + \frac{\tau^2}{2}(\hat{v}_{tt}^0)_k + O(\tau^3)$$
$$\approx (\widehat{\eta_0})_k + \tau(\widehat{\eta_1})_k + \frac{\tau^2}{2}\left\{-\alpha k^2(\widehat{\eta_0})_k + \alpha^2 k^4(\widehat{\eta_0})_k - \alpha k^2 F_k[(\eta_0)^2] - \frac{\alpha}{4}k^2 F_k[|\gamma_0|^2]\right\}, \tag{3.26}$$

Note that the spatial discretization error of the method is of spectral order accuracy in h and the time discretization error is demonstrated to be second-order accurate in τ.

4. Properties of the numerical methods

Define the usual l_2-norm:

$$\|u^n\|_{l_2} = \sqrt{\frac{2\pi}{M}\sum_{j=0}^{M-1}|u_j^n|^2}. \tag{4.1}$$

Theorem 1. *The scheme 3.19, 3.20, 3.21 for the Schrödinger–Boussinesq equation possess the following conservative properties:*

$$\|u^{n+1}\|^2 = \|u^0\|^2, \quad n = 0, 1, 2, \ldots. \tag{4.2}$$

Proof. For the scheme (3.19)–(3.21),noticing that (4.1), (3.14) and (3.15), one has

$$\begin{aligned}
\frac{1}{2\pi}\|u^{n+1}\|_{l_2}^2 &= \frac{1}{M}\sum_{j=0}^{M-1}|u_j^{n+1}|^2 = \frac{1}{M}\sum_{j=0}^{M-1}\left|\frac{1}{M}\sum_{k=-M/2}^{M/2-1}\exp\left(-\frac{3ik^2\tau}{4\varepsilon}\right)(\hat{u}^{**})_k\exp(ik\tilde{x}_j)\right|^2 \\
&= \frac{1}{M^2}\sum_{k=-M/2}^{M/2-1}\left|\exp\left(-\frac{3ik^2\tau}{4\varepsilon}\right)(\hat{u}^{**})_k\right|^2 = \frac{1}{M^2}\sum_{k=-M/2}^{M/2-1}|(\hat{u}^{**})_k|^2 = \frac{1}{M^2}\sum_{k=-M/2}^{M/2-1}\left|\sum_{j=0}^{M-1}u_j^{**}\exp(-ikx_j)\right|^2 \\
&= \frac{1}{M}\sum_{j=0}^{M-1}|u_j^{**}|^2 = \frac{1}{M}\sum_{j=0}^{M-1}\left|\exp\left[-\frac{i\tau}{4\varepsilon}\left(v_j^n + v_j^{n+1}\right)\right]u_j^*\right|^2 = \frac{1}{M}\sum_{j=0}^{M-1}|u_j^*|^2 \\
&= \frac{1}{M}\sum_{j=0}^{M-1}\left|\frac{1}{M}\sum_{k=-M/2}^{M/2-1}\exp\left(-\frac{3ik^2\tau}{4\varepsilon}\right)(\hat{u}^n)_k\exp(ik\tilde{x}_j)\right|^2 = \frac{1}{M^2}\sum_{k=-M/2}^{M/2-1}\left|\exp\left(-\frac{3ik^2\tau}{4\varepsilon}\right)(\hat{u}^n)_k\right|^2 \\
&= \frac{1}{M^2}\sum_{k=-M/2}^{M/2-1}|(\hat{u}^n)_k|^2 = \frac{1}{M^2}\sum_{k=-M/2}^{M/2-1}\left|\sum_{j=0}^{M-1}u_j^n\exp(-ikx_j)\right|^2 = \frac{1}{M}\sum_{j=0}^{M-1}|u_j^n|^2 = \frac{1}{2\pi}\|u^n\|_{l_2}^2,
\end{aligned} \tag{4.3}$$

Here, we used the identities

$$\sum_{j=0}^{M-1}\exp(i2\pi(l-k)j/M) = \begin{cases} 0, & l-k \neq mM, \\ M, & l-k = mM, \end{cases} m \text{ integer} \tag{4.4}$$

and

$$\sum_{k=-M/2}^{M/2-1}\exp(i2\pi(l-j)k/M) = \begin{cases} 0, & l-j \neq mM, \\ M, & l-j = mM, \end{cases} m \text{ integer}. \tag{4.5}$$

Thus, the equality (4.2) can be obtained from (4.3) for the scheme (3.19)–(3.21) by induction.

Before the stability analysis, we induct an useful lemma.

Lemma 1 [20]. *Suppose that λ_1 and λ_2 are the two roots of the real coefficients quadratic equation*

$$\lambda^2 - b\lambda - c = 0.$$

Then $|\lambda_1|$, $|\lambda_2| \leqslant 1$, if and only if

$$|b| \leqslant 1 - c \leqslant 2.$$

By using the von Neumann analysis for the discretization scheme (3.24), we have the stability of the scheme

Theorem 2. *When $1/4 \leqslant \beta \leqslant 1/2$, the scheme (3.24) is unconditionally stable. When $0 \leqslant \beta < 1/4$, it is conditionally stable. The stability condition is*

$$\tau \leqslant \min_{-M/2\leqslant k\leqslant M/2-1, k\neq 0} \sqrt{\frac{-4}{(1-4\beta)(\alpha^2k^4-\alpha k^2-\alpha k^2A)}}.$$

Proof. For the discretization scheme (3.24), plugging $(\hat{v}^{n+1})_k = \mu(\hat{v}^n)_k = \mu^2(\hat{v}^{n-1})_k$ into (3.24) with $|\mu|$ the amplification factor, we have the characteristic equation

$$\mu^2 + \left[\frac{-2-\tau^2(\alpha^2k^4-\alpha k^2-\alpha k^2A)(1-2\beta)}{1-\tau^2(\alpha^2k^4-\alpha k^2-\alpha k^2A)\beta}\right]\mu + 1 = 0. \tag{4.6}$$

Let $\alpha^2k^4-\alpha k^2-\alpha k^2A = z$. Not loosing the universality, assuming that $z < 0$.

According to the Lemma 1, if and only if $|\frac{2+\tau^2z(1-2\beta)}{1-\tau^2z\beta}| \leqslant 2$, then the root of the Eq. (4.6) satisfy that $|\mu_{1,2}| \leqslant 1$. Thus, when $\frac{1}{4} < \beta \leqslant \frac{1}{2}$, we have

$$\tau^2 z \leqslant \frac{-4}{1-4\beta}. \tag{4.7}$$

The (4.6) is hold for arbitrary value of τ. Therefore, in this case of $\frac{1}{4} < \beta \leqslant \frac{1}{2}$, the scheme is unconditionally stable.

When $0 \leqslant \beta < \frac{1}{4}$, we have

$$\tau^2 z \geqslant \frac{-4}{1-4\beta}. \tag{4.8}$$

This implies that

$$\tau^2 \leqslant \frac{-4}{(1-4\beta)z}. \tag{4.9}$$

Thus, the stability condition for the case $0 \leqslant \beta < 1/4$ is

$$\tau \leqslant \sqrt{\frac{-4}{(1-4\beta)z}}, \tag{4.10}$$

or

$$\tau \leqslant \min_{-M/2\leqslant k\leqslant M/2-1, k\neq 0} \sqrt{\frac{-4}{(1-4\beta)(\alpha^2k^4-\alpha k^2-\alpha k^2A)}}. \tag{4.11}$$

It is not difficult to see that the scheme is also unconditionally stable for $\beta = 1/4$. Thus we get the Theorem 2.

5. Numerical experiments

We present some numerical results of the solitary wave solutions and the plane wave solutions for the coupled Schrödinger–Boussinesq equations. The initial conditions are always chosen such that u_0, v_0 and v_1 decay to zero sufficiently fast as $|x|$ tending to the two boundary points. We choose an appropriately long interval $[a,b]$ for the computations such that the periodic boundary conditions do not introduce a significant error relative to the whole space problem.

Let u_h and v_h be the numerical solution of (3.7)–(3.11) by using the TSFS method. To quantify the numerical methods, we define some error functions as

$$e_\infty^u = \max_{k=1}^{n} \max_{j=1}^{M} \left(\left|u_{hj}^k - u(x_j,t^k)\right|\right),$$
$$e_\infty^v = \max_{k=1}^{n} \max_{j=1}^{M} \left(\left|v_{hj}^k - v(x_j,t^k)\right|\right)$$

and evaluate the conserved quantities by using the numerical solution (i.e., replacing u and v by their numerical counterparts u_h and v_h, respectively) as

$$I_u^* = \int_a^b |u_h|^2 dx,$$
$$I_v^* = \int_a^b v_h dx,$$

Here, we compute the relative errors of the three conservation quantities using the following formulations

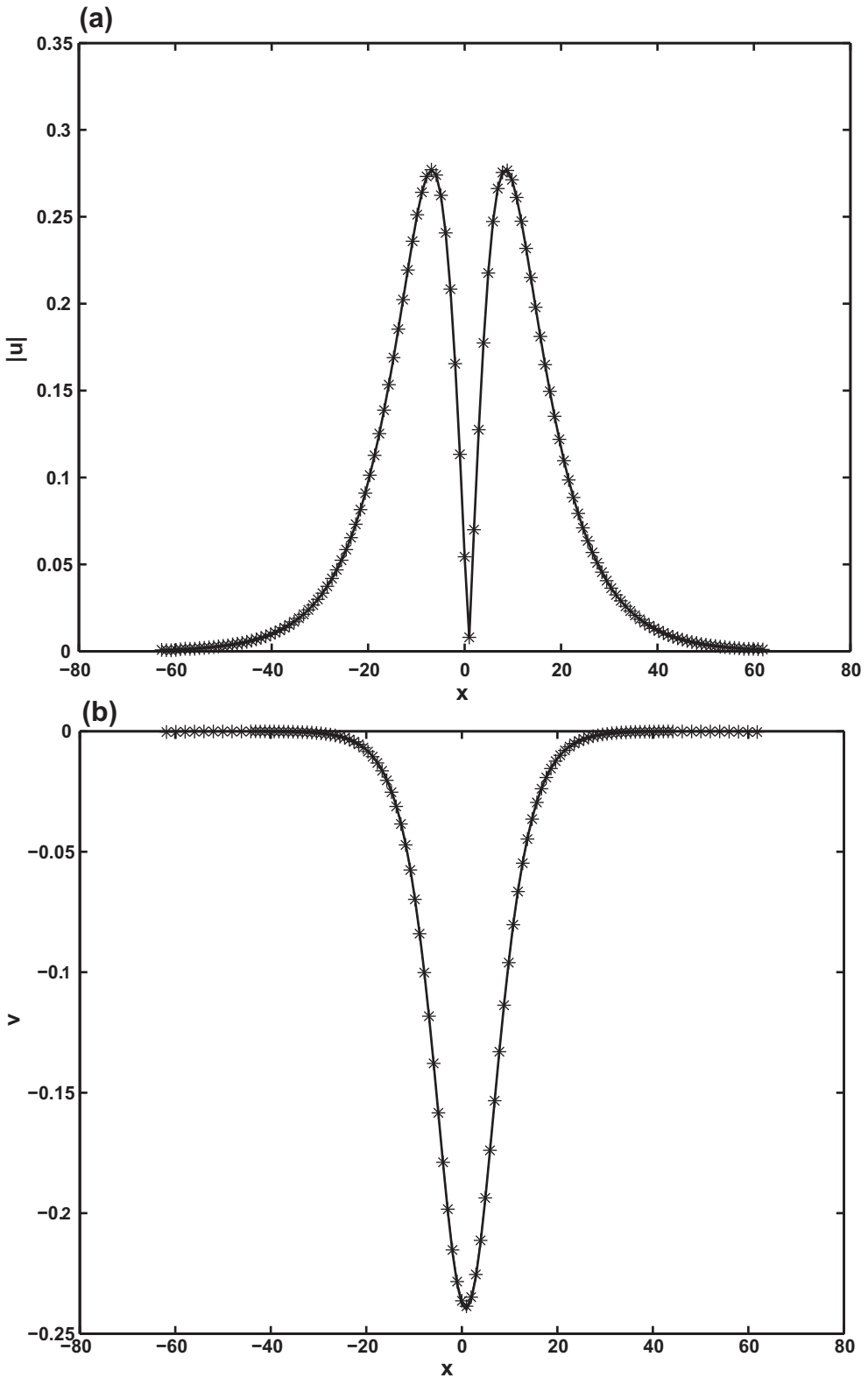

Fig. 1. The numerical solution and the exact solution of Example 1: (a) $|u|$, (b) v ('—' Exact,'$***$' Numerical) under $M = 128$, $\tau = 1/128$.

$$R_u = |I_u^*(t^n) - I_u(t^0)|/|I_u(t^0)|,$$
$$R_v = |I_v^*(t^n) - I_v(t^0)|/|I_v(t^0)|,$$
$$R_H = |I_H^*(t^n) - I_H(t^0)|/|I_H(t^0)|.$$

Example 1. The coupled Schrödinger–Boussinesq equations have the C-solitary wave solutions which are given in (2.5) and (2.6). We choose the initial conditions as following

$$\gamma_0(x) = +8\sqrt{3}\lambda \operatorname{sech}(\rho x)\tanh(\rho x)\exp(ikx), \tag{5.1}$$
$$\eta_0(x) = -6\lambda \operatorname{sech}^2(\rho x), \tag{5.2}$$

where $\rho = \sqrt{3}/15$, $\lambda = 0.04$, and $k = \sqrt{165}/45$. The initial condition $\eta_1(x)$ is taken as

$$\eta_1(x) = v_t(x,0), \quad a < x < b, \tag{5.3}$$

where $\gamma_0(x)$ and $\eta_0(x)$ are obtained from (2.5) and (2.6) by setting $t = 0$.

In this case, we solve the problem on the interval $[-20\pi, 20\pi]$, i.e., $a = -20\pi$ and $b = 20\pi$ with vanishing boundary conditions. Fig. 1 plot the evolution of the exact and the numerical solution at $t = 1$. The results shown that the curves of $|u|$ and v coincident well with the exact solutions, respectively. That is to say, our method gives a very good agreement with the exact result.

To examine the accuracy of our time-splitting method for the Schrödinger–Boussinesq equations, we perform the spatial and temporal discretization error tests (see Tables 1 and 2). The maximum error e_∞^u and e_∞^v are decreasing with the decreasing of the temporal step τ and with the increasing of the number of the node in the direction of spacial, respectively. Meanwhile, we also show the conserved quantities tests (see Table 3). From the relative error at different time, it can be seen that the two conserved quantities are well preserved with the development of time.

Example 2. The coupled Schrödinger–Boussinesq equations have plane wave solutions [19]. We choose $\varepsilon = 1$ in (3.1) and consider the problem on the interval $[a,b]$ with $a = 0$ and $b = 4\pi$. The initial conditions are taken as

$$\eta_0(x) = 1 > 0, \quad \eta_1(x) = 0, \quad \gamma_0(x) = 2\exp(ix). \tag{5.4}$$

We solve this problem by using TSFS method with mesh size $M = 128$ and temporal step size $\tau = 0.1$. Fig. 2 shows the numerical results at $t = 1$. The real and imaginary part of u are well consistent with the exact solution. Thus, our TSFS method for Schrödinger–Boussinesq equations provides the accurate plane-wave solution of the (3.1)–(3.4).

Table 1
Temporal discretization error test: at time $t = 0.5$ under $M = 128(\varepsilon = 1)$.

Time step	$\tau = 1/10$	$\tau = 1/100$	$\tau = 1/1000$
e_∞^u	2.2588395e−003	1.8769623e−003	2.3762429e−004
e_∞^v	1.3589308e−002	1.3582712e−003	1.3581335e−004

Table 2
Spatial discretization error test: at time $t = 0.5$ under $\tau = 1/10000(\varepsilon = 1)$.

Mesh size	$M = 32$	$M = 64$	$M = 128$
e_∞^u	2.8717008e−002	2.2813145e−003	2.3762431e−004
e_∞^v	2.3788234e−004	1.3300320e−004	1.3675260e−005

Table 3
Conserved quantities test: under $M = 128$, $\tau = 1/128$ $(\varepsilon = 1)$.

Time	$t = 0$	$t = 0.5$	$t = 1.0$
I_u^*	1.7736147	1.7736147	1.7736147
R_u		5.3833102e−015	6.1344697e−015
I_v^*	−4.1569178	−4.1569177	−4.1569177
R_v		1.1015694e−008	2.2381594e−008
I_H^*	1.238851	1.2388565	1.2388747
R_H		4.1448804e−006	1.8810726e−005

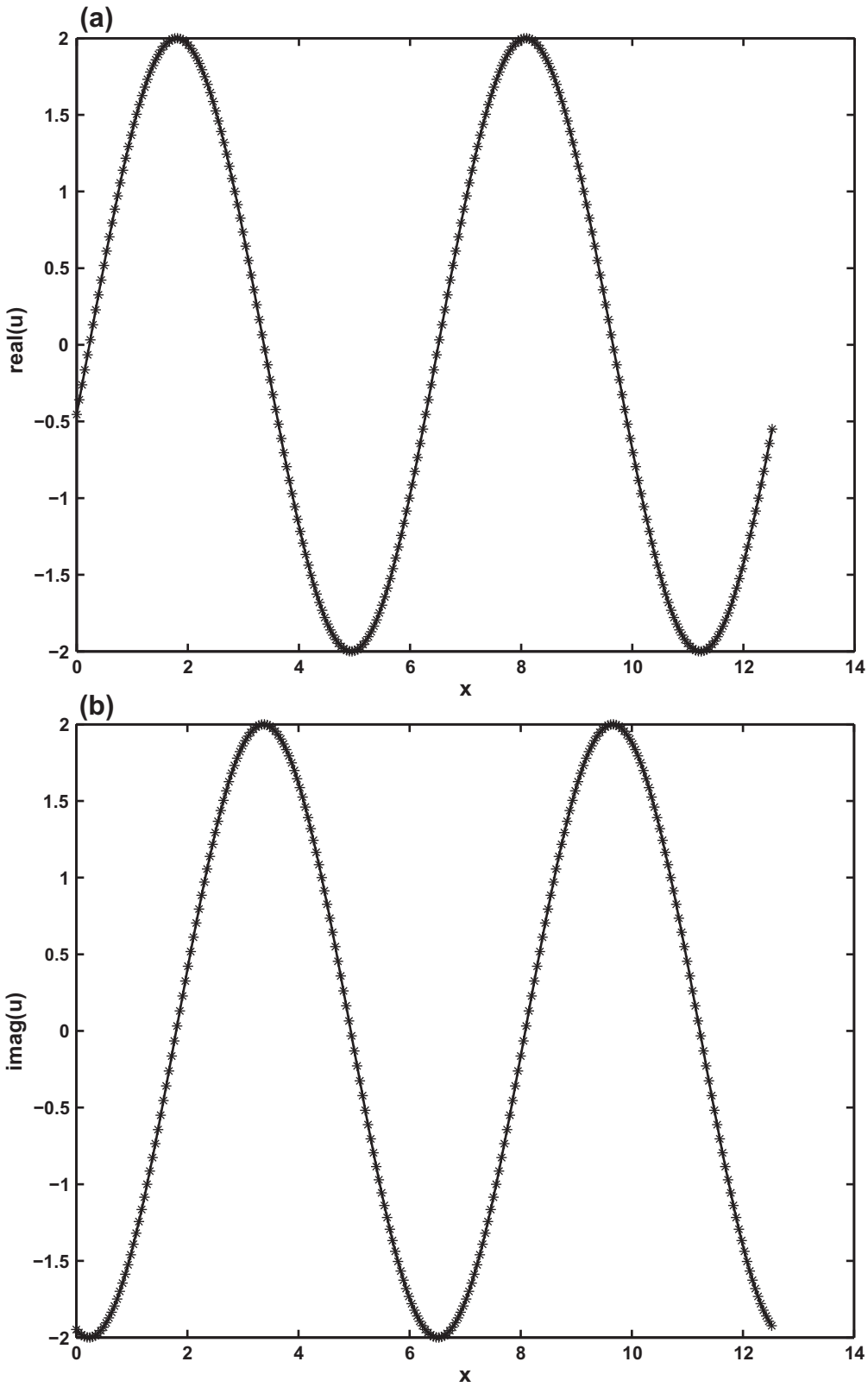

Fig. 2. The numerical solution and the exact solution of Example 2: (a) *real*(*u*), (b) *imag*(*u*) ('—' Exact,'∗∗∗' Numerical) under $M = 128, \tau = 0.1$.

6. Conclusion

We have studied the coupled Schrödinger–Boussinesq equations by the time-splitting Fourier spectral method. A comparison have been made between numerical solutions and exact solutions. Numerical experiments show that the proposed method exhibit high accuracy and efficiency.

Acknowledgments

This work has been supported by the Fundamental Research Funds for the Central Universities under Grant No. 2010QNA35.

References

[1] Makhankov VG. On stationary solutions of Schrödinger equation with a self-consistent potential satisfying Boussinesq's equations. Phys Lett A 1974;50:42–4.
[2] Rao NN. Near-magnetosonic envelope upper-hybrid waves. J Plasma Phys 1988;39:385–405.
[3] Chowdhury AR, Dasgupta B, Rao NN. Painléve analysis and Backlund transformations for coupled generalized Schrödinger–Boussinesq system. Chaos Solitons Fract 1998;9:1747–53.
[4] Saha P, Banerjee S, Chowdhury AR. Normal form analysis and chaotic scenario in a Schrödinger–Boussinesq system. Chaos Solitons Fract 2002;14:145–53.
[5] Hu XB, Guo BL, Tam HW. Homoclinic orbits for the coupled Schrödinger–Boussinesq equation and coupled Higgs equation. J Phys Soc Jpn 2003;72:189–90.
[6] Hase Y, Satsuma J. An N-soliton solution for the nonlinear Schrödinger equation coupled to the Boussinesq equation. J Phys Soc Jpn 1988;57:679–82.
[7] Rao NN. Exact solutions of coupled scalar field equations. J Phys A 1989;22:4813–25.
[8] Wang XY, Xu BC, Taylor PL. Exact soliton solutions for a class of coupled field equations. Phys Lett A 1993;173:30–2.
[9] Panigrahy M, Dash PC. Soliton solutions of a coupled field using the mixing exponential method. Phys Lett A 1999;261:284–8.
[10] Bai D, Zhang L. The finite element method for the coupled Schrödinger–KdV equations. Phys Lett A 2009;373:2237–44.
[11] Bao W, Jin S, Markowich PA. On the time-splitting spectral approximations for the Schrödinger equation in the semiclassical regime. J Comput Phys 2002;175:487–524.
[12] Bao W, Yang Li. Efficient and accurate numerical methods for the Klein–Gordon–Schrödinger equations. J Comput Phys 2007;225:1863–93.
[13] Muslu GM, Erbay HA. A split-step fourier method for the complex modified Korteweg–de Vries equation. Comput Math Appl 2003;45:503–14.
[14] Borluk H, Muslu GM, Erbay HA. A numerical study of the long wave-short wave interaction equations. Math Comput Simulat 2007;74:113–25.
[15] Vaissmoradi N, Maleka A, Momeni-Masuleh SH. Error analysis and applications of the Fourier–Galerkin Runge–Kutta schemes for high-order stiff. J Comput Appl Math 2009;231:124–33.
[16] Fornberg B, Driscoll TA. A fast spectral algorithm for nonlinear wave equations with linear dispersion. J Comput Phys 1999;155:456–67.
[17] Nishikawa K, Hojo H, Mima K, Ikezi H. Coupled nonlinear electron-plasma and ion-acoustic waves. Phys Rev Lett 1974;33:148–51.
[18] Ikezi H, Nishikawa K, Mima K. Self-modulation of high-frequency electric field and formation of plasma cavities. J Phys Soc Jpn 1974;37:766–73.
[19] Chang Q, Wong YS, Lin CK. Numerical computations for long-wave short-wave interaction equations in semi-classical limit. J Comput Phys 2008;227:8489–507.
[20] Li RH, Feng GC. The numerical methods for the differential equation. Beijing: Higher Education Press; 1997.